CONF-950472--5
SAND94-2519C

Frequency response of a TeO_2 slow shear wave acousto-optic cell exposed to radiation

Ireena A. Erteza, David C. Craft, K. Terry Stalker

Optical Systems and Image Processing Department
Sandia National Laboratories
Albuquerque, NM 87185-0843

E.W. Taylor, M.A. Kelley, A.D. Sanchez,
S.P. Chapman, D.M. Craig, E. Kinsley

AFMC Phillips Lab
Kirtland AFB, NM 87117

ABSTRACT

Radiation testing of photonic components is not new, however component level testing to date has not completely addressed quantities which are important to system behavior. One characteristic that is of particular importance for optical processing systems is the frequency response. In this paper, we present the results of the analysis of data from an experiment designed to provide a preliminary understanding of the effects of radiation on the frequency response of acousto-optic devices. The goal is to present possible physical mechanisms responsible for the radiation effects and to discuss the effects on signal processing functionality.

The experiment discussed in this paper was designed by Sandia National Laboratories (SNL) and performed by SNL and Phillips Laboratory (PL) personnel at White Sands Missile Range (WSMR). In the experiment, a TeO_2 slow shear-wave acousto-optic cell was exposed to radiation from the WSMR linear accelerator. The TeO_2 cell was placed in an experimental configuration which allowed swept frequency diffracted power measurements to be taken during radiation exposure and recovery. A series of exposures was performed. Each exposure consisted of between 1 to 800, 1 μsec radiation pulses (yielding exposures of 2.25 kRad(Si) to 913 kRad(Si)), followed by recovery time.

At low total and cumulative doses, the bandshape of the frequency response (i.e. diffracted power vs. frequency) remained almost identical during and after radiation. At the higher exposures, however, the amplitude and width of the frequency response changed as the radiation continued, but returned to the original shape slowly after the radiation stopped and recovery proceeded. It is interesting to note that the location of the Bragg degeneracy does not change significantly with radiation. In this paper, we discuss these effects, and we discuss the effect on the signal processing functionality.

1 INTRODUCTION

Optical processing has been around for more than a quarter of a century. Although it has not become universally accepted, optical processing has shown itself to be useful in a variety of situations. Some of the advantages of optical processing systems include high speed, a large capacity for handling data, compact and light weight systems, and low power. Recent improvements in various optical and optoelectronic devices are

making optical processing even more attractive for certain applications. One of these applications is space-based optical processing, where size and power are critical. However, the effects of radiation are a concern for space applications and must be quantified.

The goal of this paper is to address the effect of radiation on acousto-optic cells being used in optical processing systems. To this end, SNL designed an experiment to measure the frequency response of an acousto-optic cell; the experiment, itself, is a very simple processing system–a spectrum analyzer.

A spectrum analyzer was chosen because it is a simple processing configuration, however, it contains virtually all the components that are in more complicated processing systems. The basic configuration of a spectrum analyzer is shown in Figure 1.[2] Its operation can be explained as follows.

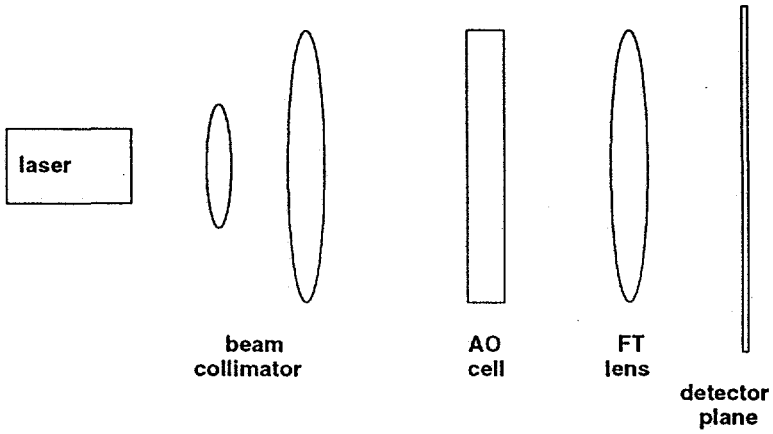

Figure 1: Basic Layout of a Spectrum Analyzer

Light from a laser is expanded and collimated to fill the aperture of an acousto-optic (AO) cell. The RF signal applied to the cell acts as a moving diffraction grating for the collimated light. The light is diffracted by the sound column at angles proportional to the frequency components of the RF signal supplied. The intensity at the different angles indicates the amount of RF power at that corresponding frequency. A lens can be placed behind the cell to capture and focus the light onto a detector array, located at what can be called the frequency plane. Since the diffracted angle out of the AO cell is proportional to the frequency, the various positions in the detector array correspond to various frequencies.

The behavior of such a spectrum analyzer can be described mathematically as follows. The collimated, expanded light source illuminates the AO cell with a spatial distribution $f(x)$. Typically, this distribution is a truncated gaussian. The RF input to the transducer creates a traveling acoustic wave inside the cell $g(x-Vt)$, where V is the velocity of sound in the cell. The result of the acousto-optic interaction is proportional to $f(x)g(x-Vt)$. The diffraction efficiency of the acousto-optic cell varies with the frequency of the acoustic wave inside the cell. Let this variation be described by $B(f_x)$, where f_x is the acoustic spatial frequency. The lens following the AO cell performs a fourier transform, such that the output, $O(x')$ is given by

$$O(x') = B(x') \cdot \left[F(x') * G(x')e^{j2\pi x'Vt}\right] = B(x') \int_0^\infty f(\xi)g(\xi - Vt)e^{-2\pi j x'\xi} d\xi, \qquad (1)$$

where x' is the coordinate in the output plane. The term $e^{j2\pi x'Vt}$ is a Doppler shift, due to the velocity of sound. The output of the photodetector is then proportional to $|F(x') * G(x')|^2$, assuming the Bragg frequency response of the AO cell, $B(f_x)$, is flat over the band of interest. Since the fourier transform of a broad function in time is narrow in frequency spectrum, it is clear that the frequency resolution of the system is limited by the aperture of the cell, which directly affects $f(x)$. Because optical processing is based on linearity and superposition, the frequency response of AO cells is of critical concern.

2 EXPERIMENTAL CONFIGURATION

SNL has a project with the Defense Nuclear Agency (DNA) called Radiation Effects on Optical Processing Systems (REOPS). The goal of this project is to relate component level radiation effects to system level performance through modeling and testing of a selected optical processing system. This goal requires the identification of a "generic" architecture which incorporates key features of most optical processing systems to serve as a basis for the modeling effort. The acousto-optic spectrum analyzer architecture described previously was chosen as a prototypical optical processing system, because it has all the major components of most optical processing systems. With the test system chosen, work is proceeding toward the project goal: to test the behavior of the individual components exposed independently to radiation and determine how those radiation effects can affect system performance. The acousto-optic cell is critical to many acousto-optic processing systems, hence we are concentrating on the effects on this component first.

The experimental configuration for the prototypical optical system (acousto-optic spectrum analyzer) is shown in Figure 2. The parts in this figure are numbered, and the numbers refer to the items listed in Table 1.

Light is provided by a HeNe laser with a neutral density filter. The output power after the filter is 580μW. A special mount for the AO cell was built. The mount enables rotation about the acoustic axis (y-axis [110]) and about the x-axis running perpendicular to the plane including [110] and the optical rail path. A stop is placed on the cylindrical lens to block out the DC and negative diffraction orders. The tilt of the detector face is very critical, because at certain angles, the face of the detector can send a reflected beam back into the laser, altering the beam characteristics.

Table 1: Optical Parts

Part No.	Item Description
1	Uniphase 1135P HeNe laser, 20 mW, linearly polarized
2	NRC 811 laser mount
3	NRC 370 post assembly
4	counterweight
5	1.47 neutral density filter, reflective type
6	Oriel Dog to secure plate to optical rail
7	Newport #38 plate (12.6cm X 7.5 cm)
8	Newport linear translator stage
9	Newport 360-90 triangle bracket
10	Newport 481 series rotary stage
11	Custom mount for AO cell
12	AO cell
13	Melles Griot 78803 #10 cylindrical lens; focal length 150 mm
14	Melles Griot 10 nm bandpass interference filter centered at 632.8 nm
15	Pin 10 silicon detector, 1 cm in diameter

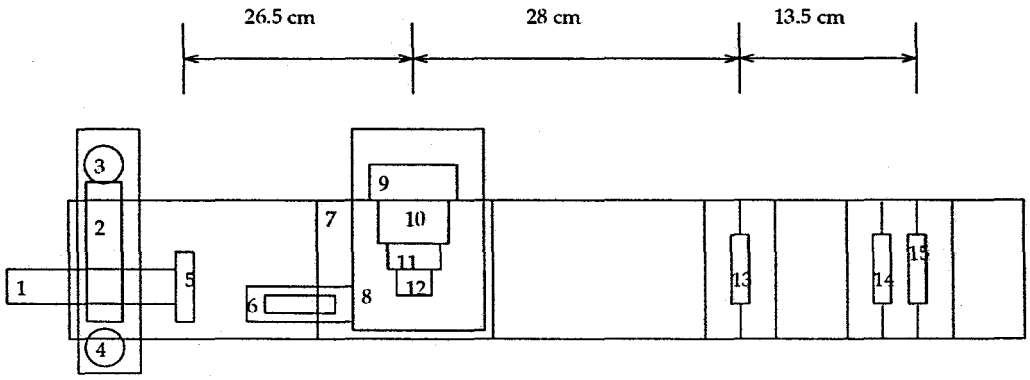

Figure 2: Top View of Experiment on an Optical Rail

Figure 3 shows the corresponding electronics for this experiment. The numbered parts are listed in Table 2. The electronic spectrum analyzer and oscilloscope were used for monitoring purposes; they are not part of the AO spectrum analyzer system. Measurements were taken to quantify the frequency response of the various

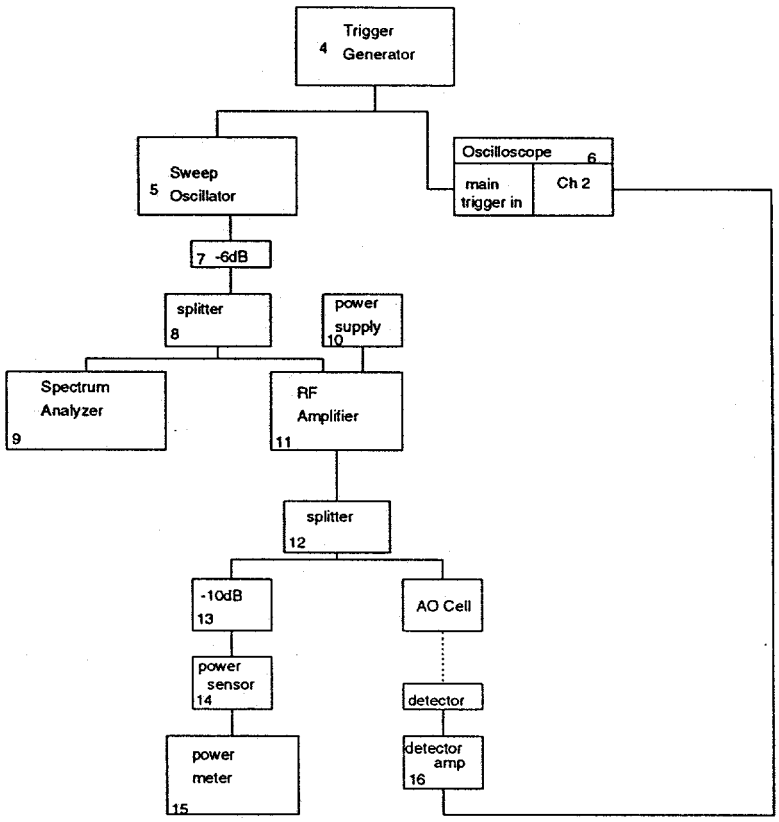

Figure 3: Block Diagram of Electronics

Table 2: Electrical Parts

Part No.	Item Description
4	Wavetek Model # 134 Sweep Generator
5	HP 8620C Sweep Oscillator
6	Tektronix 7854 Oscilloscope
7	6dB RF attenuator
8	MiniCircuits 50-50 splitter
9	Tektronix 496P Programmable Spectrum Analyzer
10	BK Precision DC power supply; 30V, 1 ampere
11	MiniCircuits ZHL-2-8 RF Power Amplifier
12	MiniCircuits 50-50 splitter
13	10dB RF attenuator
14	HP 8482A Power Sensor
15	HP 436A Power Meter
16	Melles Griot Large Dynamic Amplifier

RF amplifiers. The RF amplifiers used in this experiment were chosen to have a reasonably flat response in the band of interest. The variations in the band of interest were within 10% for all the amplifiers used.

The configuration in Figures 2 and 3 was designed, built and tested in a radiation-free environment at SNL. Testing included checking the general operation of the system and characterization of the system. In addition, the acousto-optic interaction plane was rotated to give a flat, wide frequency response, with the location of the Bragg degeneracy clearly visible. The RF frequency was swept from 12–65 MHz. RF power was 400 mW. Nominal characteristics for the Crystal Tech AO cell are 30 MHz bandwidth, centered at 50 MHz, with a 70μsec time aperture. The clear aperture measures 12 mm $\times$ 43.5 mm. Once this testing was done, with the system robustly mounted on a portable optical rail, the experiment was taken to WSMR and exposed to radiation.

3 EXPERIMENTAL RESULTS

This section shows plots of the experimental results. The radiation source was from the WSMR Linac. The energy of the electron beam was nominally 15 MeV, and the pulse duration of each pulse was 1 μsec. The pulse repetition rate was 30 Hz, or equivalently every 33 msec. Dosimeters were placed to get a dose reading in kRad (Si), and thermistors were placed to monitor the temperature variation of the cell. These data are shown in the following plots and table. On the plot legends, the subscripts refer to the trace number. Traces were taken sequentially during and after radiation.

Table 3: Dose Information

Exposure #	# Pulses	Dose (kRad (Si))	Cumulative Dose (kRad (Si))
1	1	2.25	2.25
2	5	11.25	13.5
3	20	40.9	54.4
4	50	95.1	149.5
5	75	79.9	229.4
6	100	105.4	334.8
7	100	157.5	492.3
8	200	209.2	701.5
9	400	434.0	1144.0
10	400	434.0	1578.0
11	600	667.0	2715.1
12	800	913.4	3628.43

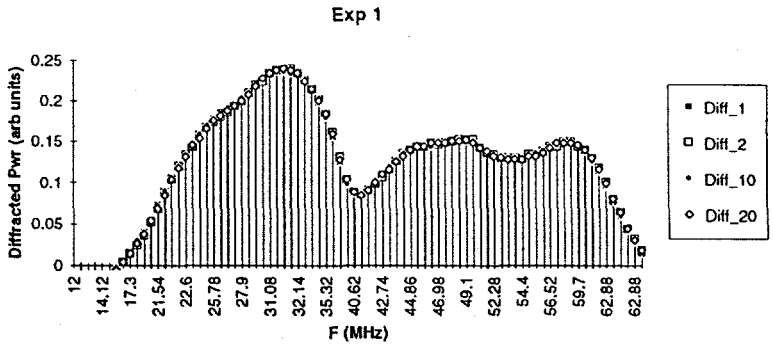

Figure 4: Exposure 1: Trace 1 was after the first and only radiation pulse. Traces 2, 10 and 20 were during the recovery period.

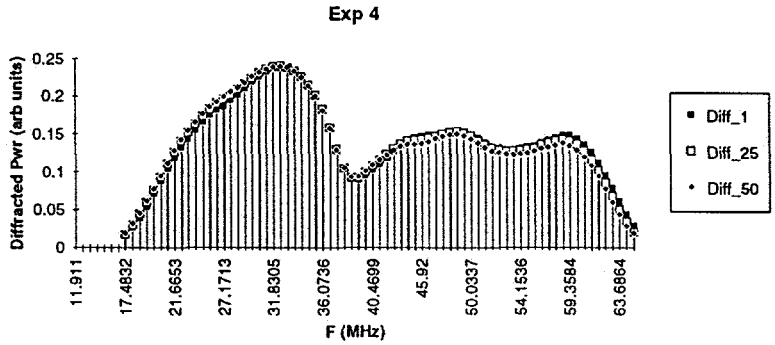

Figure 5: Exposure 4, Plot 1: Traces 1, 25 and 50 were during radiation.

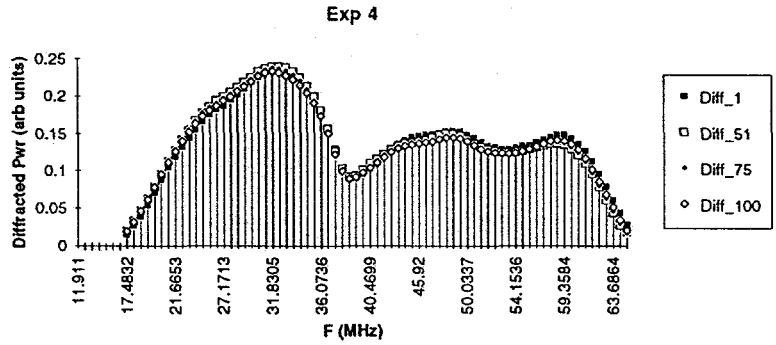

Figure 6: Exposure 4, Plot 2: Traces 51, 75 and 100 were during recovery.

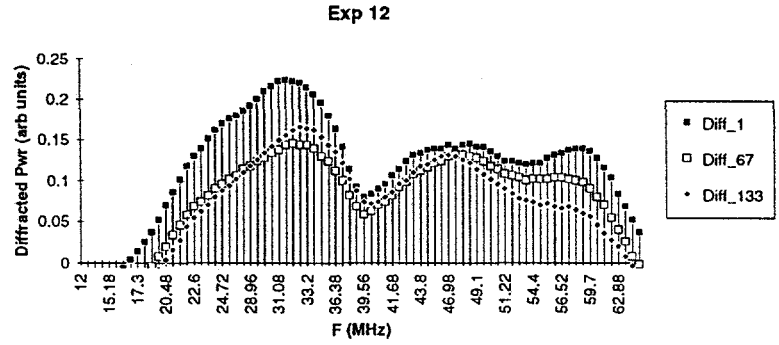

Figure 7: Exposure 12 Plot 1: Traces 1, 67 and 133 were during radiation.

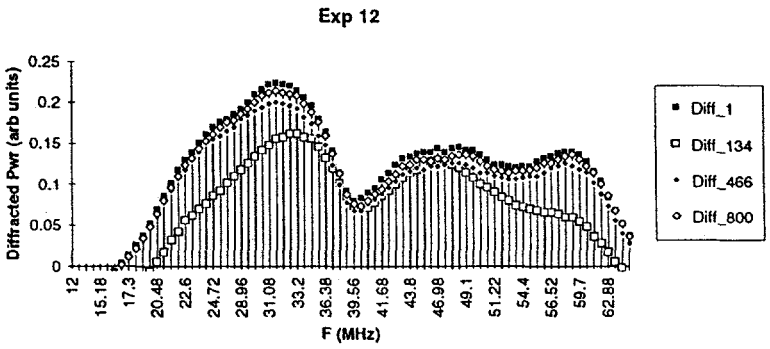

Figure 8: Exposure 12 Plot 2: Traces 134, 466 and 800 were during recovery.

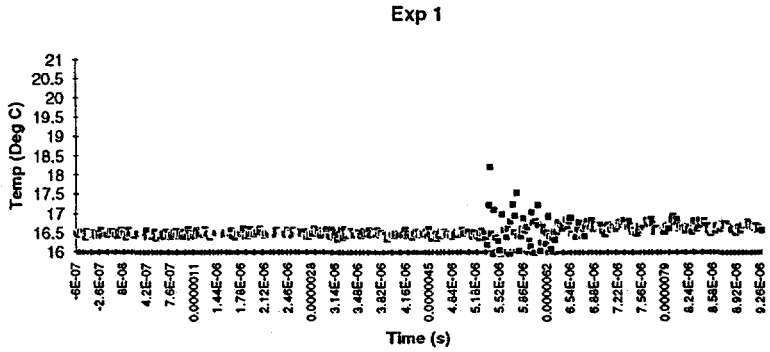

Figure 9: Exposure 1

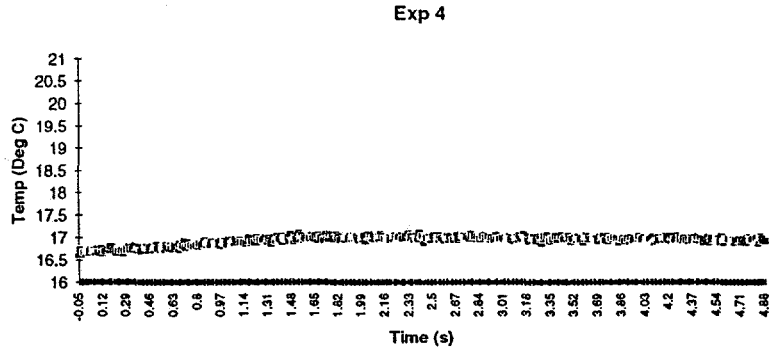

Figure 10: Exposure 4

4 DISCUSSION

From looking at the data in the previous section, we can make some generalizations about the effect of these levels of radiation on an acousto-optic cell. At low total and cumulative doses, the frequency response bandshape (i.e. diffracted power vs. frequency) remained almost identical during and after radiation. Exposure 4 (95.1 kRad (Si)) is where very slight changes start to be noticed. The accompanying maximum temperature variation for this exposure is 0.4°C. At higher exposures, changes in the bandshape are more noticeable. The frequency response changes as the radiation continues, but returns to the original shape after the radiation stops and recovery proceeds. The temperature data also shows the same type of excursion; the temperature rises as the radiation continues, but starts to return back to the original temperature exponentially after

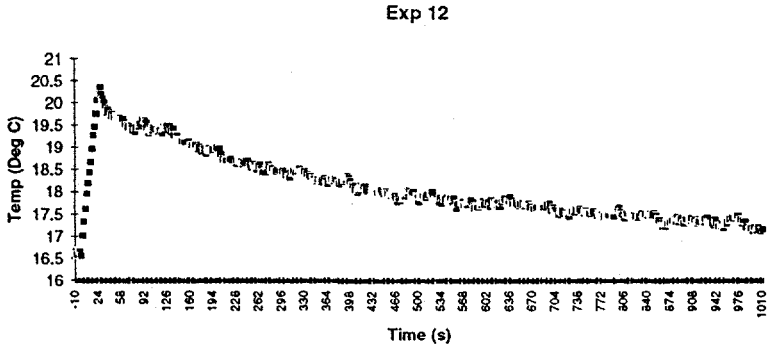

Figure 11: Exposure 12

the radiation stops. The maximum change in frequency response bandshape corresponds with the maximum heating.

The changes in frequency response can be broken into three parts: (1) the location of the Bragg degeneracy; (2) the 3-dB bandwidth of the diffracted beam intensity; and (3) the bandshape of the diffracted beam intensity. These items were investigated thoroughly in an attempt to determine the mechanisms that cause changes in them with radiation.[10] Here, we present the conclusions of that analysis.

4.1 Location of Bragg Degeneracy

To begin, let us first briefly describe the Bragg degeneracy. For more detail, a number of references may be consulted.[10,27,15,6] If the fast mode of light is incident upon the acoustic wave vector, such that the diffracted beam is in the slow mode and is perpendicular to the acoustic wave vector, a degeneracy occurs at a certain frequency. This frequency is the location of the Bragg degeneracy. The degeneracy means that there are two angles which satisfy the pseudomomentum conservation. As a result, some light is deflected into the undesired, degenerate mode, causing a dip in the first order diffracted beam power at the given frequency. There is usually some divergence associated with the acoustic wave, which gives the dip a certain width. This is a phenomenon associated with tangential phase matching.

The change in location of the Bragg degeneracy observed in this experiment can be attributed entirely to the increase of temperature of the cell with radiation.

4.2 3-dB Bandwidth of Diffracted Beam Intensity

In looking at the plots of the diffracted beam intensity vs. frequency, it is hard to discern the effect on the bandwidth. By bandwidth, we mean the span of frequency over which the diffracted power remains within a certain tolerance, usually 3-dB. It can be shown that the 3-dB bandwidth in anisotropic bragg diffraction is a function of L, the crystal interaction length. Using thermal expansion coefficients,[17] the change in 3-dB bandwidth due to thermal expansion can be calculated. The change in 3-dB bandwidth due to thermal expansion for the temperature variation in this experiment is virtually non-existent. Consequently, changes in 3-dB bandwidth are attributed to a change in acoustic power and/or acoustic attenuation. It is well known[23,25] that the acoustic attenuation for a crystal like TeO_2 is proportional to the frequency squared, $\alpha = \alpha_0 f^2$. Consequently if the acoustic attenuation constant, α_0, increases, the higher frequency components will be attenuated more, and the bandwidth will decrease.

4.3 Bandshape of Diffracted Beam Intensity

The data shows that the bandshape of the frequency response changes with radiation. Briefly, the changes can be described as: (1) The overall diffraction efficiency (diffracted power) is reduced; (2) The reduction of diffracted power varies with frequency, with the difference between the diffracted power in the low frequency peak and the high frequency peak decreasing; and (3) Through Exposure 8, as one would expect, with more radiation, the diffracted power was uniformly lower than without radiation for all frequencies. At Exposure 10, the performance is slightly better at higher frequency with higher radiation exposure, and the two peaks are approaching the same height. At Exposure 11, at maximum radiation, the two peaks are virtually identical in height, and the degeneracy dip has decreased. At Exposure 12, the low frequency peak increased to be once again higher than the high frequency peak. At Exposures 11 and 12, a severe rolloff at highest frequencies is seen.

The changes in bandshape can also be attributed to changes in acoustic power, P_a, and acoustic attenuation. Because no material studies have been done to establish the dependence of acoustic attenuation on temperature, it cannot be determined if the change in α is due to the radiation itself, or the temperature rise due to radiation. This must be studied further.

The observed changes in frequency response can be related to system performance. Though the magnitude of changes do not appear that great, they do impact the performance achievable with acousto-optic processing systems. This will be discussed further in a Section 4.5.

4.4 Recovery from Effects

The exposures in this experiment ranged from 2.25 kRad (Si) to 913 kRad (Si). All of the effects we have discussed appear to be transient, i.e. not permanent. It is clear that after the radiation pulses stop, the frequency response starts to go back to its original characteristics. Although data was not always taken out to the time of complete recovery, complete recovery did occur between runs. Note that the temperature recovery corresponds to the frequency response recovery.

4.5 Effect on Signal Processing Functions

It is interesting to see in the previous sections how radiation affects the frequency response of an acousto-optic cell, but the critical issue is how the signal processing performance is affected when the AO cell is used in an optical processing system. More specifically, we are interested in how the performance of an AO spectrum analyzer will be affected by radiation.

For most AO processing systems, a critical parameter is the time bandwidth product (TBWP) of the AO cell. The TBWP, often described by the variable N, is given by $\tau\Delta f$, where τ is the transit time across the cell, and Δf is the maximum bandwidth of the device. The TBWP can be thought of as the information capacity of the cell, and hence the system. Equivalently, the TBWP is the number of resolvable elements. By resolvable elements, we mean either the number of resolvable frequencies in a fourier transform plane or the number of resolvable elements in an image plane. The TBWP is determined by the maximum duration and bandwidth signal on which the device can properly operate. An increase in TBWP means either an increase in interaction time, an increase in interaction bandwidth, or both.

In the previous sections, we have seen that a variety of physical parameters are affected by radiation or temperature. These parameters, in turn, affect the TBWP and hence the performance of an AO processing system. Recall, that as the cell is radiated, it heats up. Consequently, the acoustic velocity increases.[18,5] This increase in V will limit τ, the transit time across the cell, and hence the TBWP. Recall $\tau = D/V$, where D is the cell aperture. In addition, we infer that with radiation, P_a decreases. A possible cause of this is increased acoustic attenuation with temperature or with radiation. An increase in attenuation limits the allowable cell aperture, and hence also limits τ.

In applications where the speed of the deflector is not of major concern, the resolution is limited by either the physical constraint of the optical aperture or the acoustic attenuation, α, at high frequency. Both these items serve to limit D. (If speed is of concern, that too limits D, usually more so than the physical constraint or acoustic attenuation.) For most crystalline solids, the acoustic attenuation is proportional to the frequency squared, $\alpha = \alpha_0 f^2$. If the maximum attenuation tolerated is $\mathcal{L}$ (dB), then the maximum allowed transit time would be $\frac{\mathcal{L}}{\alpha_o f_{max}^2}$. Consequently, the maximum TBWP, N_{max} is given by

$$N_{max} = \frac{\mathcal{L}\Delta f}{\alpha_o f_{max}^2}. \tag{2}$$

It is clear that if the acoustic attenuation increases, with either temperature or radiation, the maximum number of resolvable points decreases accordingly.

Work must be done to investigate acoustic attenuation. Acoustic absorption vs. temperature for shear [100] has been presented.[17] Indeed there is an increase with temperature, of about $\frac{1}{150}\frac{dB/cm}{^\circ C}$, but this cannot be guaranteed to occur or at what magnitude for shear [110]. If increased acoustic attenuation can be attributed solely to the increase in temperature, then temperature stabilization can be used to take care of the limits imposed from increased acoustic velocity and attenuation on the TBWP. If the decrease in P_a cannot be attributed to increased temperature alone, then even with temperature stabilization, the TBWP will decrease, and the processing capacity will be reduced with radiation.

Temperature stabilization has already been shown to be necessary for acousto-optic spectrum analyzers.[5] The acoustic velocity has a direct affect on frequency resolution,

$$\Delta f = \frac{sV}{\lambda F},$$

where s is the spacing between detectors in the detector array, and F is the focal distance of the lens. For a TeO_2 cell (slow shear mode [110]), with bandwidth of 60MHz, center frequency of 90MHz, and time aperture of $70\mu s$, it was shown that temperature must be stabilized to within $0.328^\circ C$ to maintain the highest TBWP (N=4200). If the detector spacing is relaxed and the full TBWP is not utilized, the ΔT restrictions can be lessened. For N=1000, $\Delta T < 1.39^\circ C$.

Finally if the magnitude of the signal at a given frequency is important, not just detection, then some sort of compensation or equalization is typically required. This type of compensation is commonly done using electronic pre- or post-processing. If it is known that the bandshape may vary and the various bandshapes are known a priori, it wouldn't be difficult to incorporate this into the electronic compensation. Of course, all the electronic processing would be implemented using hardened components.

5 CONCLUSION

In this paper, we presented the results of an experiment designed to show the effect of space-level radiation on the frequency response of a TeO_2 slow shear acousto-optic cell. Possible mechanisms responsible for the changes observed were presented, and the changes were related to overall system performance.

At low total and cumulative doses, the frequency response bandshape remained almost identical during and after radiation. Slight changes began to be noticed at a dose of 95.1 kRad (Si) and got larger with increasing dose. The frequency response changed as the radiation continued, but returned to the original shape after the radiation stopped and recovery proceeded. Accompanying the radiation and changes in frequency response was an increase in temperature.

The changes in frequency response can be broken into three parts: (1) the location of the Bragg degeneracy; (2) the 3-dB bandwidth of the diffracted beam intensity; and (3) the bandshape of the diffracted beam intensity.

These three items were investigated thoroughly.[10] The change in location of the Bragg degeneracy can be attributed entirely to the increase of temperature of the cell with radiation. The change in 3-dB bandwidth due to thermal expansion is virtually non-existent. Consequently, changes in 3-dB bandwidth are attributed

to a change in acoustic power and/or acoustic attenuation. The changes in bandshape can also be attributed to changes in acoustic drive power and acoustic attenuation. Because no material studies have been done to establish the dependence of acoustic attenuation on temperature, it cannot be determined if the change in α is due to the radiation itself, or the temperature rise due to radiation. This must be studied further.

Finally, the observed changes in frequency response were related to system performance. Though the magnitude of changes do not appear that great, they do impact the performance achievable with acousto-optic processing systems. The effects observed will result in a reduced TBWP for the system. A reduced TBWP reduces the information processing capacity of a system, but the system can still perform.

An acousto-optic processing system operating in space must be designed so that it can perform within certain tolerances (changes in temperature within a given range, acoustic power, P_a, within a given range, acoustic attenuation within a given range, etc.). These restrictions will limit the processing capacity (or resolution), but provide a margin of safety for known correct operation under these conditions.

6 ACKNOWLEDGEMENTS

This work supported by the Defense Nuclear Agency under WFO Proposal Number 91930113 and by the United States Department of Energy under Contract DE-AC04-94AL85000. The first authors acknowledge Phillips Lab members for their part in helping to conduct the experiments at WSMR.

7 REFERENCES

[1] M. Amano, G. Elston, and J. Lucero. Materials for large time aperture Bragg cell. *SPIE Proceedings*, 567:141–149, 1985. Advances in Materials for Active Optics.

[2] N. Berg and J. Lee, editors. *Acoutsto-optic Signal Processing: Theory and Implementation.* Dekker, 1983.

[3] I. Chang. Acoutooptic devices and applications. *IEEE Transactions on Sonics and Ultrasonics*, SU23(1):2–22, January 1976.

[4] P. Das and C. DeCusatis. *Acousto-optic Signal Processing: Fundamentals and Applications.* Artech House, 1991.

[5] T. Dimmick, D. Satorius, and J. Fewer. Temperature sensitivity of acoustic velocity and frequency registration in acousto-optic spectrum analyzers. *Applied Optics*, 31(14):2409–2411, 10 May 1992.

[6] R. Dixon. Acoustic diffraction of light in anisotropic media. *IEEE Journal of Quantum Electronics*, QE-3(2):85–93, February 1967.

[7] G. Elston. Optically and acoustically rotated slow shear bragg cells in TeO_2. Technical report, Crystal Technology Incorporated, 1986.

[8] G. Elston, M. Amano, and J. Lucero. Material tradeoff for wideband Bragg cells. *SPIE Proceedings*, 567:150–158, 1985. Advances in Materials for Active Optics.

[9] G. Elston and P. Kellman. The effects of acoustic nonlinearities in acousto-optic signal processig systems. Technical report, ESL Incorporated, 495 Java Drive, Sunnyvale, CA 94088-3510.

[10] I. Erteza. Analysis of the frequency response of TeO_2 slow shear wave acousto-optic cell exposed to radiation. SAND Report SAND 95-0500, Sandia National Laboratories, P.O. Box 5800, Albuquerque, NM 87185-0843, April 1995.

[11] E. Gordon. A review of acoustooptical deflection and modulation devices. *Applied Optics*, 5(10):1629–1639, October 1966.

[12] M. Gottlieb, C. Ireland, and J. Ley. *Electro-optic and Acousto-optic scanning and Deflection.* Decker, 1983.

[13] D. Hecht. Spectrum analysis using acoutso-optic devices. *SPIE Proceedings*, 90:148–157, 1976. Acousto-Optics.

[14] B. Javidi and J. Horner, editors. *Real-Time Optical Information Processing.* Academic Press, 1994.

[15] A. Korpel. *Acousto-optics.* Dekker, 1988.

[16] K. McCarthy and H. Sample. Thermal conductivity of a fluorozirconate glass and tellurium dioxide single crystals. *14th Annual Symposium on Optical Materials for High Power Lasers.*

[17] Y. Ohmachi and N. Uchida. Temperature dependence of elastic, dielectric and piezoelectric constants in TeO_2 single crystals. *Journal of Applied Physics*, 41(6):2307–2311, May 1970.

[18] Y. Ohmachi and N. Uchida. Acoustic and acousto-optical properties of TeO_2 single crystal. *Review Electronic Communications Lab*, 20:529–541, 1972.

[19] J. Pellegrino, L. Harrison, and N. Berg. Ruggedization and miniaturization of real-time acousto-optic correlators and spectrum analyzers. *SPIE Proceedings*, 639:160–166, 1986. Optical Information Processing II.

[20] P. Phariseau. On the diffraction of light by progressive supersonic waves. *Proceedings of the Indian Academy of Sciences*, 44A:165–170, October 1956.

[21] J. Rouvaen, M. Ghazaleh, E. Bridoux, and R. Torguet. On a general treatment of acousto-optic interactions in linear anisotropic crystals. *Journal of Applied Physics*, 50(8):5472–5477, August 1979.

[22] M. Shah and D. Pape. A generalized theory of phased array Bragg interaction in a birefringent medium and its application to TeO_2 for intermodulation product reduction. *SPIE Proceedings*, 1704:210–220, 1992. Advanced in Optical Information Processing V.

[23] N. Uchida. Acoustic attenuation in TeO_2. *Journal of Applied Physics*, 43(6):2915–2917, June 1972.

[24] N. Uchida and N. Niizeki. Acoustooptic deflection materials and techniques. *Proceedings of the IEEE*, 61(8):1073–1092, August 1973.

[25] N. Uchida and Y. Ohmachi. Elastica and photoelastic properties of TeO_2 single crystal. *Journal of Applied Physics*, 40(12):4692–4695, November 1969.

[26] A. Warner, D. White, and W. Bonner. Acousto-optic light deflectors using optical activity in paratellurite. *Journal of Applied Physics*, 43(11):4489–4495, November 1972.

[27] J. Xu and R. Stroud. *Acousto-Optic Devices: Principles, Design and Applications*. J. Wiley and Sons, 1992.

[28] T. Yano, M. Kawabuchi, A. Fukumoto, and A. Watanabe. TeO_2 anisotropic Bragg light deflector without midband degeneracy. *Applied Physics Letters*, 26(12):689–691, June 1975.

[29] E. Young and S. Yao. Design considerations for acousto-optic devices. *Proceedings of the IEEE*, 69(1):54–64, January 1981.

DISCLAIMER